

Mapping Posets Into Low Dimensional Spaces: The Case of Uranium Trappers

Nancy Y. Quintero^{1,2}, Rainer Bruggemann³, Guillermo Restrepo^{1,4}

¹Laboratorio de Química Teórica, Universidad de Pamplona, Colombia

²Universidad de Antioquia, Universidad Pontificia Bolivariana and Universidad Católica de Oriente, Colombia
ytrioradiac@gmail.com

³Leibniz - Institute of Freshwater Ecology and Inland Fisheries, Department Ecohydrology, Berlin, Germany
brg_home@web.de

⁴Bioinformatics Group, Department of Computer Science, Leipzig University, Germany
grestrepo@unipamplona.edu.co; guillermo@bioinf.uni-leipzig.de

(Received December 7, 2017)

Abstract

Analysing order relationships among objects is central for decision making processes or for optimisation, which are also relevant in the field of chemistry. A mathematical tool to carry out ordering studies is the Hasse diagram technique, whose Hasse diagram summarises a large amount of order information. However, when the number of objects is large, the huge amount of intersecting lines showing order relations hinder its interpretation. In this work, we introduce the concept of posetic coordinates for objects to order and explore different mappings from them to one-, two- and three-dimensional spaces. These mappings reduce the complexity of the original Hasse diagram and are suitable for interpreting the order structure of the set of objects. The mappings here reported are applied to 83 microorganisms used for trapping uranium in contaminated aqueous systems. The results show that *Bacillus licheniformis* ATCC 14580, is the unique highly dominating species; this confirms its importance as optimal uranium trapper and highlights its usefulness for the development of biosorption procedures in environments polluted with this actinide.



1 Introduction

When it comes to order objects based on their attributes, for example for decision making processes in chemistry and environmental sciences,^{[1],[11],[2],[3],[4]} a suitable tool is the Hasse Diagram Technique (HDT), whose foundations are in order theory. A customary outcome of the HDT is a Hasse diagram, where order relationships are depicted as links between couples of objects and whose visual inspection is informative, e.g. indicating optimal or least objects.^[5]

However, HDT has constraints of practicability due to loss of interpretability with increasing number of objects;^[6] leading to multitude of intersecting lines, not visually informative.

To solve this shortcoming, the FOU plot has been devised,^{[7],[8]} which takes into account the incomparabilities and comparabilities for the objects under study. Comparabilities are order relationships among objects of the sort more reactive than, less aromatic than, for example, and incomparabilities are the lack of those relationships. In spite of the versatility of the FOU plot, its mathematical properties have not been extensively studied. In the current paper we carry out such a study and show that the FOU plot corresponds to a particular mapping of Hasse diagrams into low dimensional spaces, where also ranking procedures are included. We applied the mappings to a set of 83 microorganisms used to

2 Materials and methods

2.1 Basics on posets

If X is a non-empty set of objects, a partially ordered set can be obtained by endowing X with an order relation \preceq , which fulfils reflexivity ($x \preceq x \forall x \in X$), antisymmetry (if $x \preceq y$ and $y \preceq x$, for $x, y \in X$, then $x = y$) and transitivity (if $x \preceq y$ and $y \preceq z$ then $x \preceq z$, for $x, y, z \in X$).^[5] The couple (X, \preceq) is called a partially ordered set (*poset*).

In a poset any pair of objects $x, y \in X$ can be compared whenever $x \preceq y$ or $y \preceq x$, in those cases x and y are said to be *comparable* ($x \perp y$), otherwise they are *incomparable*, i.e. $x \not\preceq y$, $y \not\preceq x$ ($x \parallel y$).^[5]

Based on comparabilities and incomparabilities, some useful terms for the ensuing discussion are:

Definition 1. Let $x \in X$. We call $C(x)$ the set of *comparable objects* of x that is given by:
 $C(x) := \{y \in X: x \preceq y \text{ or } y \preceq x\}$.

Definition 2. Let $x \in X$. We call $I(x)$ the set of *incomparable objects* of x and it is given by:

$$I(x) := \{ y \in X : y \parallel x \}.$$

Definition 3. Let $x \in X$. We call $F(x)$ the *principal order filter* of x or *principal up set* of x and it is given by:

$$F(x) := \{ y \in X : x \leq y \}.$$

Definition 4. Let $x \in X$. We call $O(x)$ the *principal order ideal* of x or *principal down set* of x and it is given by:

$$O(x) := \{ y \in X : y \leq x \}.$$

Definition 5. For $y \in X$, given a poset (X, \leq) , if $X_i \subseteq X$, then $C(X_i) = \{ y : y \perp x, x \in X_i \}$.

We say that $(C(X_i), \leq)$ is a *local poset* of (X, \leq) .

Definition 6. A poset (X, \leq) is called a *linear order* (total order) if every pair of objects from X is comparable in \leq .

Note that a linear order meets reflexivity, antisymmetry, transitivity and linearity, i.e. $x \leq y$ or $y \leq x$ for all $x, y \in X$.^[9]

Definition 7. A poset (X, \leq) is called a *weak order* if \leq is transitive and meets linearity.

Hence, the difference between weak and total order is that the former is not antisymmetric but the latter is.

Definition 8. A *ranking* of X is a two-step procedure where 1) a weak order is found for X and 2) an ordinal (rank) is assigned to each object of X .

Definition 9. A *component* of a poset (X, \leq) is a local poset (Definition 5) $(C(X_i), \leq)$ of (X, \leq) such that the cardinality of $C(X_i)$ is maximal.

A traditional approach to explore the order relations in (X, \leq) is through the visualisation of the associated Hasse diagram (HD), which is a directed acyclic transitive-reduced graph whose vertices are objects in X and the edges indicate a cover relation between the two connected vertices. It is said that x is “covered” by y if there is no object z with $x < z$ and $z < y$.

Other posetic concepts needed for the discussion are those of maximal, minimal and isolated objects. “Posetic” is used throughout this paper for describing partial order features inherent to objects in a poset without necessarily extracting information just from the HD.

A *maximal object* x is an object for which no relation $x \preceq y$ is found.^{[5],[10]} Conversely, a *minimal object* x is an object for which no relation $y \preceq x$ is established. *Isolated objects* are maximal and minimal objects at the same time.^{[5],[10]}

A particular posetic approach to order objects based on their attributes is the Hasse diagram technique^[1], where objects of X are characterised by a set of attributes. These attributes are further used to compare objects and in consequence need to be rightly oriented to indicate the same evaluation aim.

2.2 Posetic space and posetic cases of interest

We use $F(x)$, $O(x)$ and $I(x)$ as proxies for the order information of the object x of the poset (X, \preceq) .

We represent the cardinality of X by $|X|$ and for the sake of simplicity $|C(x)| = C$, $|F(x)| = F$, $|O(x)| = O$ and $|I(x)| = I$. Likewise, $|X| = X$. An important property is that $F(x)$, $O(x)$ and $I(x)$ are functions.

Proposition 1. There is a function $f: X \rightarrow (|F(X)|, |O(X)|, |I(X)|)$.

Proof: For all $x \in X$ there is only one $F(x)$, therefore only one $|F(X)|$. Likewise holds for $|O(X)|$ and $|I(X)|$ ■

From Definitions 2 to 4, Theorem 1 follows:

Theorem 1. $F + O + I = X + 1$.

Proof: Every object $x \in X$ has $|X|$ possible order relationships, which are distributed into comparabilities $C(x)$ and incomparabilities $I(x)$. Thus:

$$C(x) + I(x) = X \tag{1}$$

As comparable objects y are exclusively above ($x \preceq y$) or below ($y \preceq x$), then for $x \in F(x)$ and $x \in O(x)$:

$$C(x) = F + O - 1 \tag{2}$$

Therefore, by replacing (2) in (1) and by further rearranging it is obtained:

$$F + O + I = X + 1 \blacksquare$$

We introduce the posetic coordinates to characterise objects by their order attributes.

Definition 10: We call $P(x) = (|F(x)|, |O(x)|, |I(x)|)$ the *posetic coordinates* of any $x \in X$ of the poset (X, \preceq) . For simplicity we write them as (F, O, I) .

Proposition 2. The upper and lower bounds of F , O and I are: $1 \leq F \leq X$, $1 \leq O \leq X$ and $0 \leq I \leq X - 1$.

Proof: By Definition 3 the minimum number of objects belonging to any filter of $x \in X$ is 1, i.e. the object x . Likewise, by Definition 4 the minimum cardinality of O is 1. By definitions 3 and 4, the maximum number of objects either in F or in O is the complete set of objects, therefore their upper bound is X . By Definition 2 it follows that the minimum number of incomparable objects for any $x \in X$ is 0, where $x \perp y$, for all $y \in X$. In contrast, the maximum number of incomparable objects for $x \in X$ is $X - 1$, where $x \parallel y$, for all

$y \in X \setminus x$, where $X \setminus x$ means the set X without the element x ■

Definition 11. The Cartesian product $F \times O \times I$ is called the *posetic space*.

Some particular regions of such a space have extreme distributions of posetic coordinates and some others result from internal symmetries of the coordinates. Besides the sort of coordinates' distributions, these regions bring interesting order information about the objects located there. We define these regions through the posetic cases of interest.

Definition 12. We call *posetic cases of interest* (PCI) the points of the posetic space with the following features of their posetic coordinates:

Case A: $\max F$

Case B: $\max I$

Case C: $\max O$

Case D: $F = I$

Case E: $O = I$

Case F: $F = O$

Case G: $F = O = I$

A closer look to the posetic coordinates of PCIs shows that they are only realised as shown in Corollary 1.

Corollary 1. For a given poset (X, \preceq) , the posetic cases of interest are realised through the following posetic coordinates:

$$A (\max F) = (X, 1, 0)$$

$$B (\max I) = (1, 1, X-1)$$

$$C (\max O) = (1, X, 0)$$

$$D (F = I) = \begin{cases} D1 = ([X/2], 1, [X/2]) \text{ or} \\ D2 = ([X/2], 1, [X/2]) \end{cases}$$

$$E (O = I) = \begin{cases} E1 = (1, [X/2], [X/2]) \text{ or} \\ E2 = (1, [X/2], [X/2]) \end{cases}$$

$$F(F=O) = \begin{cases} F1 = \left(\left\lfloor \frac{|X+1|}{2} \right\rfloor, |X| - \left\lfloor \frac{|X+1|}{2} \right\rfloor + 1, 0 \right) \text{ or} \\ F2 = \begin{cases} \left(|X| - \left\lfloor \frac{|X+1|}{2} \right\rfloor + 1, \left\lfloor \frac{|X+1|}{2} \right\rfloor, 0 \right), \text{ for even } |X| \text{ and} \\ \left(\frac{|X+1|}{2}, \frac{|X+1|}{2}, 0 \right), \text{ for odd } |X| \end{cases} \end{cases}$$

$$G(F=O=I) = (|X|/3, |X|/3, |X| - 2|X|/3 + 1)$$

The different floor $\lfloor \cdot \rfloor$ and ceiling $\lceil \cdot \rceil$ functions result from the necessity of bringing fractions to the natural numbers to realise the PCIs as actual points of the posetic space. The deduction of these expressions is shown in the Appendix (Propositions A1 to A4). Figure 1 exemplifies the PCIs for $|X|=4$ and $|X|=5$.

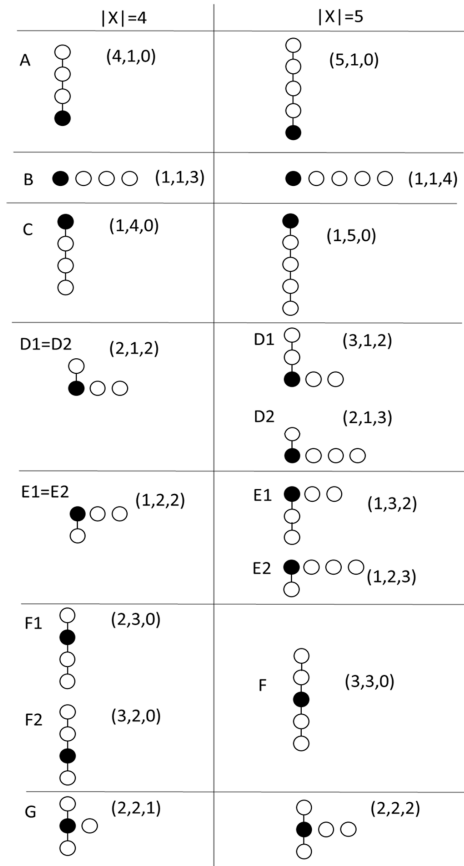


Figure 1. Posetic cases of interest from A to G for $|X|=4$ and $|X|=5$ and some Hasse diagrams realising them. Triples correspond to (F, O, I) .

2.3 Mappings from posetic coordinates

The introduction of posetic coordinates makes that any x of a poset can be mapped to the space $P(x)$. Here we discuss the exploration of such a space by applying three different mappings.

- (1) Three dimensional: $i: P(x) \rightarrow P(x)$.
- (2) Two dimensional: $FOU: P(x) \rightarrow (|F(x)| - |O(x)|, |I(x)|)$.
- (3) One dimensional: $r: P(x) \rightarrow r(x) = \frac{|O(x)|(X-1)}{|O(x)+F(x)|}$.

2.3.1. Three dimensional mapping (ternary space)

This mapping corresponds to the identity mapping $i:(F, O, I) \rightarrow (F, O, I)$, which corresponds to a ternary space (ternary plot)^[11] (Fig. 2). Based on their posetic coordinates, objects can be located in the ternary plot.

This plot is a barycentric one depicting three variables (F, O, I) whose sum yields a constant value ($X + 1$) that is usually represented as 100%. Because of Theorem 1, the coordinates are not independent, so only two coordinates must be known to find a point on the graph. Each point in the ternary space is a triple of the cardinality of the three sets $F(x), O(x)$ and $I(x)$. The advantage of using a ternary space for depicting posetic features is that the three posetic coordinates can be conveniently plotted in a two-dimensional graph, without loss of information.

The posetic coordinate I grows from 0 to 100% from the bottom of the plot to the upper apex, labelled I . The horizontal lines that represent various percentages of I run parallel to the base line.

The posetic coordinate F grows from the right side of the triangle (side of apexes I and O) to the leftmost apex, labelled F . The parallel lines to the side opposite to the apex F characterise the degree of F . Similarly, the values of O can be read from the lines opposite to the apex O . Although the ternary space gives a theoretical framework to plot each $x \in X$ of a poset (X, \preceq) , the actual area of the ternary space that can be populated by (F, O, I) of X is lower.

Proposition 3. In a ternary space (F, O, I) any $x \in X$ is plotted in the following working subspace:

$$\frac{100}{X + 1} \leq F \leq \frac{100X}{X + 1}$$

$$\frac{100}{X+1} \leq O \leq \frac{100X}{X+1}$$

$$0 \leq I \leq \frac{100(X-1)}{X+1}$$

Proof: If $X + 1$ corresponds to 100% for F , O and I , then the corresponding upper and lower bounds of F, O, I (Proposition 2) lead to

$$\frac{100}{X+1} \leq F \leq \frac{100X}{X+1}$$

$$\frac{100}{X+1} \leq O \leq \frac{100X}{X+1}$$

$$0 \leq I \leq \frac{100(X-1)}{X+1} \blacksquare$$

Fig. 2 γ shows the ternary plot for $|X| = 5$ and depicts the posetic cases of interest, PCI, of Fig. 1 as well as the objects of a toy-example HD shown in Fig. 2 α .

2.3.2. Two dimensional mapping (FOU space)

The working subspace of the ternary space has strong connections with the so-called FOU space, where in the original paper^{[7],[8]} the notation U was used instead of I .

In the FOU space the definition of axes is carried out by using the difference between subsets $O - F$ for the abscissa and I for the ordinate. $O - F > 0$ when x has more objects y holding $y \preceq x$ than $x \preceq y$, i.e. more objects below than above in a HD. It is $O - F < 0$ for the contrary case and equal to zero when the number of objects below and above is the same. Note that in the ternary plot the posetic coordinates are given by percentages of $X + 1$, while in the FOU space they are treated as the bare numbers they bring, i.e. (F , O , I).

Proposition 4. In the FOU space $1 - X \leq O - F \leq X - 1$.

Proof: The upper bound of $O - F$ is met when O is maximum (X) and F minimum (1) (Proposition 2), then $\max(O - F) = X - 1$.

The lower bound results when O is minimum (1) and F is maximum (X), then $\min(O - F) = 1 - X \blacksquare$

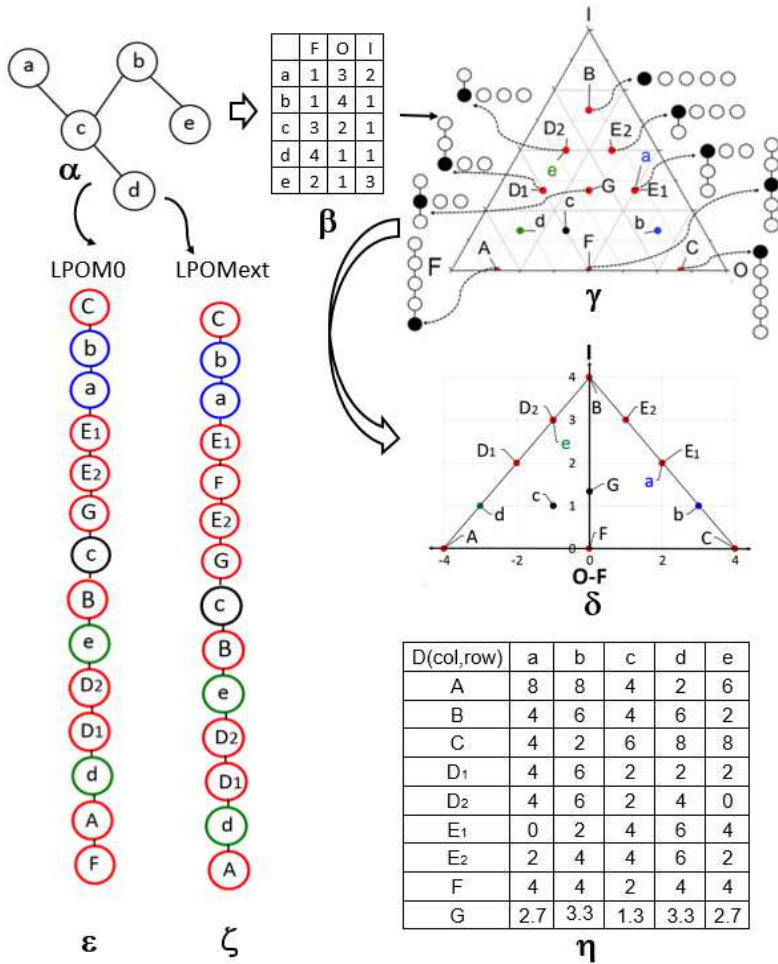


Figure 2. α) Toy example HD for $|X|=5$, β) posetic coordinates of objects in α , γ) ternary plot for objects a to e in α , depicting the posetic cases of interest (PCIs) (Fig. 1) δ) FOU space for objects in α and the placement of the PCIs, ϵ) LPOM0 and ζ) LPOMext for α where the PCIs are also depicted. η) Manhattan distances between the objects in α (columns) and the PCIs (rows). Further explanations on some of subfigures α - η will come in further sections.

Proposition 5. The FOU space is bounded by $I = O - F + X - 1$, for $O - F \leq 0$; by $I = F - O + X - 1$, for $O - F \geq 0$ and by $I = O$.

Proof: For $O - F \leq 0$; from Proposition 4 $\min(O - F) = 1 - X$. From Proposition 4 and Theorem 1, $O - F$ values corresponds to $I = 0$, which builds the point $(1 - X, 0)$ of the FOU space.

In $O - F \leq 0$, the maximum value I can attain is its maximum, i.e. $I = X - 1$, which by Theorem 1 corresponds to $F + O = 2$. As $\min F = 1$ and $\min O = 1$, $F + O = 2$ can only be attained by $F = 1$ and $O = 1$, i.e. $O - F = 0$. Hence, $\max I$ corresponds to the point $(0, X - 1)$ of the FOU space.

The line connecting $(1 - X, 0)$ with $(0, X - 1)$ has slope:

$\frac{X-1}{X-1} = 1$, therefore its equation is $I = O - F - (1 - X)$, being $1 - X$ the $O - F$ intercept.

Hence, $I = O - F + X - 1$.

For $O - F \geq 0$, Proposition 4 shows that $\max(O - F) = X + 1$. From Proposition 4 and Theorem 1, $\max(O - F)$ corresponds to $I = 0$. This makes the point $(X - 1, 0)$ of the FOU space.

In $O - F \geq 0$ the maximum value I can take is $X - 1$, which as shown for $O - F \leq 0$ corresponds to $(0, X - 1)$.

The line connecting $(0, X - 1)$ with $(X - 1, 0)$ has slope $-\frac{X-1}{X-1} = -1$, therefore its equation is $I = -(O - F) + X - 1 = F - O + X - 1$ ■

Proposition 6. In the FOU space the posetic cases of interest have coordinates $(O - F, I)$:

$$A: (-(X - 1), 0)$$

$$B: (0, X - 1)$$

$$C: (X - 1, 0)$$

$$D: \left(-\frac{X - 1}{2}, \frac{X - 1}{2}\right)$$

$$E: \left(\frac{X - 1}{2}, \frac{X - 1}{2}\right)$$

$$F: (0, 0)$$

$$G: \left(0, \frac{X - 1}{3}\right)$$

Proof: They are obtained from Theorem 1 and Proposition 4.

Fig. 2γ and 2δ show that the FOU space is a subspace of the ternary plot. The advantage of using the ternary plot is that the three posetic coordinates are depicted, while in the FOU space two are combined. The advantage of the FOU space over the ternary plot is

that the whole space is reachable by objects of a poset of the given cardinality, whilst in the ternary plot a fraction of the space is unreachable.

In both, ternary plot and FOU space, the nearness of the objects of a given poset to the posetic cases of interest can be calculated, e.g. through a metric; such a measure can be used as a proxy to assess the order relationships of the objects. Here we use the Manhattan distance¹, whose results for Fig. 2 are shown in Fig. 2η.

To better interpret the results of Fig. 2η, the local HD, as a depiction of a local poset (Definition 5), of each object in Fig. 2α is shown (Fig. 3). Note how the original HD for *b*, is equivalent to *b'*, in terms of their (*F*, *O*, *I*), likewise occurs for *c* and *c'*, and *d* and *d'*.

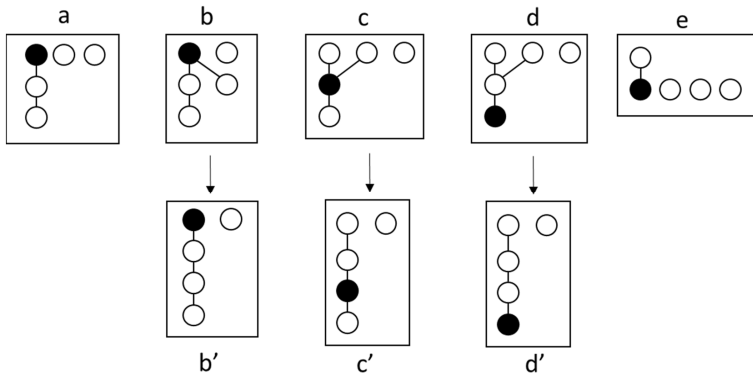


Figure 3. Local Hasse diagrams (*a* to *e*) of objects in the diagrams of Fig. 2α and the (*F*, *O*, *I*) equivalent diagram *b'*, *c'*, *d'* regarding *b*, *c*, *d*, respectively.

From Fig. 2η it is quantified what is observed in Fig. 2γ and 2δ: the equivalence of *a* with *E1* and of *e* with *D2*, the tie of *b* with *E1* and *C* (better understood through *b'* (Fig. 3) and of *d* (or *d'*) with *A* and *D1* and the nearness of *c* (or *c'*) with *G*. This can be interpreted as: *a* is exactly the case of an evenly dominating and incomparable object. Whilst *b* is dominating but with incomparabilities. The object with the most balanced comparabilities, up and down, and incomparabilities is *c*. In turn, *d* is close to be

¹ As J. D. MacCuish and N. E. MacCuish discuss in reference [12], the suitable similarity measure must be selected based upon the kind of data, e.g. binary, count, continuous and mixed. Taking into account the discrete character of the data we have, we used the Manhattan distance, which avoid continuous geometrical assumptions of the space.

maximally dominated, which is hampered by incomparabilities. In fact d and e are the two instances of objects evenly dominated and incomparable.

In general, minimal objects lay over the line connecting PCI A with B on the FOU plot and maximal objects over the line BC. The line AC contains those objects with no incomparabilities. A broad interpretation of the FOU plot is shown in Fig. 4.

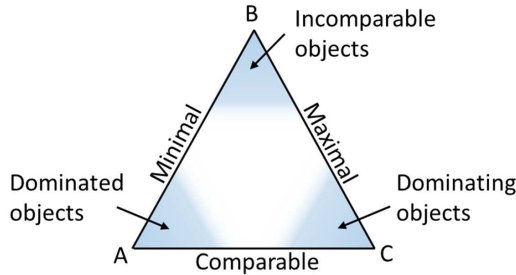


Figure 4. Regions of the FOU space depicting important order information.

2.3.3. One-dimensional mapping (ranking)

This is the most popular mapping, which reduces the whole complexity of order relationships of a poset to a single number, i.e. a rank in a ranking (Definition 8). Here, each $x \in X$ is associated to its rank average r , whose calculation takes into account the comparabilities and incomparabilities of x to estimate its position (rank) in a one-dimensional scale. In this approach, objects x holding $x \preceq y$ for many y receive low ranks while those having many y of the sort $y \preceq x$ receive high ranks. Bruggemann and coworkers have devised methods to compute rank averages^{[13],[14]} and in the current paper two variants of the local partial order model LPOM approaches are used: LPOM0 and LPOMext. LPOM0 is calculated as follows:

$$r(x) = \frac{|S(x)|+1)*(X+1)}{X+1-|I(x)|}$$

Where $S(x)$ is the set of successors of x , which corresponds to $O(x) \setminus x$. From Theorem 1:

$$r(x) = \frac{|O(x)|*(X+1)}{|O(x)+F(x)|} \tag{3}$$

The respective expression for LPOMext is:

$$r(x) = |O(x)| + p$$

Where p depends on:

$$p_y^< = |O(x) \cap I(y)| \text{ and } p_y^> = |F(x) \cap I(y)|, \text{ with } y \in I(x).$$

Hence, any object in $I(x)$ contributes to $r(x)$ according to its probability of being positioned below. Thus, the sum is performed over $\frac{\rho_y^<}{\rho_y^< + \rho_y^>}$.^[13] Therefore

$$r(x) = |O(x)| + \sum_{y \in I(y)} \frac{p_y^<}{p_y^< + p_y^>} \tag{4}$$

As a rule of thumb, maximal elements often have large values for $|O(x)|$, therefore their average ranks values tend to be large too, due to Equations 3 and 4.

Fig. 2ε and 2ζ show the rankings for LPOM0 and LPOMext. It is seen how, in general, $c > b > a > c > e > d$. As in both methods O is the dominating term (Equations 3 and 4), objects with high O attain high rankings and objects in subsequent ranks start to appear as O is reduced and F and I start to increase.

Fig. 2ε and 2ζ also depict the nearnesses of Fig. 2η, e.g. that d is in between A and DI shows up as $DI > d > A$.

2.4 Microorganisms for U trapping

After having described the mathematics of the mappings, in this section we apply them to the ordering of 83 microorganisms used for uranium (U) trapping.

In a recent study, Quintero et al.^[4] ordered 38 microorganisms for U trapping characterising these objects by three attributes: percentage of U removal ($\%U$); uptake capacity (UC) and the requested time (t) for removing U input. In the current study we analyse a bigger set of species reported in the literature for U trapping in aqueous systems by including 45 additional bacteria.

The U uptake capacity was assessed through the same attributes as reported by Quintero, Bruggemann and Restrepo^[4]: $\%U$, UC and eff , this latter being t oriented in such a way that large eff values indicate better U recovering (details in reference [4]).

3 Results and discussion

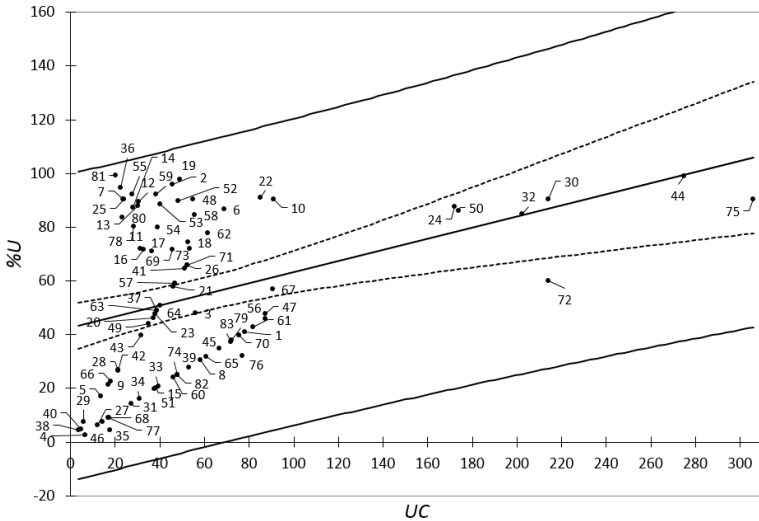
3.1 Attributes' statistics

We analysed the association between pairs of attributes in ordinal measurement levels by Spearman's correlation coefficients ρ (Fig. 5α). Fig. 5α shows that there is a moderate and positive correlation between $\%U$ and UC ; ρ for $\%U$ and eff and UC and eff

indicate a weak and positive correlation in the monotonic relationship between these attributes.

ρ	%U	UC
%U	1.0	0.404
UC	0.404	1.0
<i>eff</i>	0.260	0.286

α)



β)

Figure 5. α) Spearman correlation coefficients for attributes %U, UC and *eff*. β) Regression chart of %U by UC, showing 1) points corresponding to 83 microorganisms as labelled in Table A1 (Supplementary material); 2) the regression line (best linear fit); 3) 95% prediction interval for the line (continuous lines) where 95% of all data point fall; 4) 95% confidence interval on mean of the prediction for a given value of UC (dashed lines), where it has a 95% of probability of containing the true regression line; and 5) observed values (black dots). Diagonally rightward, close to 0, an angular pattern is enclosed by two rays emanating from object 38; the upper ray contains 19 objects and the lower one 23. These objects share the same value in *t* and %U ≤ 66.

To determine the degree of linear association between %U and UC, a linear regression analysis was carried out. Fig. 5β shows that there are no outliers for both the 95% prediction and confidence intervals, but there is a high variability at low UC (1-100 mg U/g biomass).

As seen from the slopes, changes in the predictor variable UC are associated with changes in the response variable $\%U$; approximately above 100 mg U/g biomass. The width of the 95% confidence interval for the expected value of UC increases as $\%U$ moves away. This means that there is approximately more certainty in the prediction of UC below 100 mg U/g biomass; additionally, from $R^2 = 0.146$, it is concluded that UC only explains 14.6% of $\%U$ variability and therefore by the regression neither $\%U$ nor UC can mutually be replaced. Therefore for the posetic analysis all three attributes are needed simultaneously.

3.2 Generalities of the ordering of microorganisms

Table A1 (Supplementary material) shows the presence of values not clearly defined for $\%U$ and eff for some microorganisms, namely 7, 10, 25, 30, 48 and 75. These microorganisms have intervals in attributes UC and eff . In the current study, microorganisms having $\%U > 90$ and $0 \leq eff \leq 1$ were set up to $\%U = 90.5$ and $eff = 1$ (see reference [4]).

In Fig. 6, the HD of 83 microorganisms is depicted, where two well-defined regions or components (Definition 9) are shown.

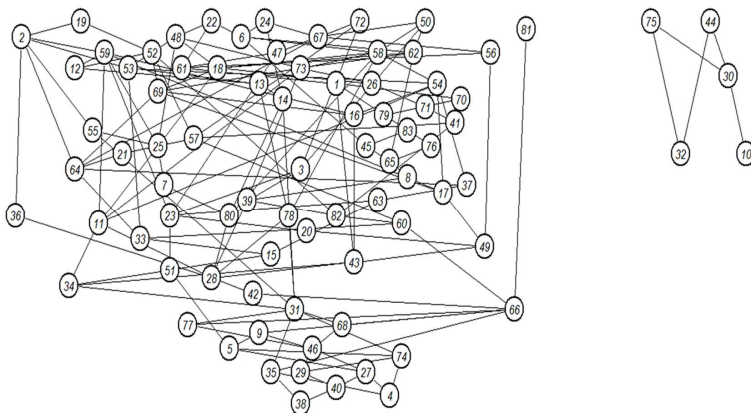


Figure 6. Hasse Diagram of 83 species. Left side: component with 78 microorganisms; right side: component with five species.

Components: By checking Table A1 (Supplementary material), it can be seen that, typically, microorganisms in the right component are characterised by very low values for eff but pretty large values for UC , whereas microorganisms in the large leftward component have higher values in eff but low values for UC . Thus, the ordinal

representation of the attribute space by a Hasse diagram reveals some important insights in the suitability of microorganism for trapping Uranium.

Maximal objects: At the top of the Hasse diagram eight maximal objects are found: *Bacillus subtilis* IAM 11062 (19), *Bacillus licheniformis* ATCC 14580 (22), *Bacillus mucilaginosus* ACCC 10012 (24), *Pseudomonas aeruginosa* J007 (44), *Pseudomonas* MGF-48 (50), *Streptomyces* sp. (72), *Sphingomonas* sp., Strain BSAR-1 (75) and *Streptomyces viridochromogenes* HUT 6167 (81).

Minimal objects: The least suitable microorganisms as U trappers are shown at the bottom: *Arthrobacter cireus* IAM 1660 (4), *Citrobacter* N14 (10), *Deinococcus radiodurans* DrPhoN (32) and *Micrococcus varians* IAM 13594 (38).

3.3 Mappings from posetic attributes of microorganisms

3.3.1. Ranking of microorganisms

When ranks are derived based on each attribute alone, some objects will heavily change their position in the ranking. Therefore, it is to be expected that these objects will heavily depend on weights in a weighted linear sum (as the simplest technique for an aggregation). Table A2 (Supplementary material) in the appendix shows this dependence on the selection of weights.

Results of the application of the two LPOM-methods are shown in Table 1.

Table 1. Average ranks for microorganisms calculated from LPOM-methods

Rank	Microorganism label		Average ranks, r (microorganism label)	
	LPOM0	LPOMext	LPOM0	LPOMext
1	22	22	82.73 (22)	82.38 (22)
2	24	24	82.64 (24)	81.99 (24)
3	50	50	82.62 (50)	81.85 (50)
4	19	19	82.35 (19)	81.33 (19)
5	72	72	82.21 (72)	80.51 (72)
6	48	48	80.89 (48)	79.79 (48)
7	2	2	80.27 (2)	77.92 (2)
8	6	6	79.24 (6)	77.71(6)
9	81	67	78.40 (81)	74.61 (67)
10	59	52	77.00 (59)	73.62 (52)
11	52	62	76.85 (52)	73.50 (62)
12	67	58	76.70 (67)	73.41 (58)

13	3	59	75.87 (3)	71.50 (59)
14	58	47	75.60 (58)	70.41 (47)
15	62	56	75.43 (62)	69.82 (56)
16	47	44,75*	74.00 (47)	66.9 (44,75)
17	56	73	73.50 (56)	66.85 (73)
18	55	18	73.04 (55)	66.37 (18)
19	53	53	71.71 (53)	66.00 (53)
20	36	3	70.74 (36)	64.40 (3)
21	73	61	70.00 (73)	63.76 (61)
22	18	55	69.70 (18)	61.15 (55)
23	61	1	67.61 (61)	60.50 (1)
24	44,75*	26	67.20 (44,75)	60.17 (26)
25	1	71	65.56 (1)	57.07 (71)
26	26	70	64.91 (26)	55.75 (70)
27	12,71*	12	63.00 (12,71)	54.26 (12)
28	70	54	62.46 (70)	54.16 (54)
29	41	69	61.09 (41)	54.05 (69)
30	54	41	60.90 (54)	53.96 (41)
31	76	79	60.67 (76)	52.04 (79)
32	25	81	60.48 (25)	52.02 (81)
33	79	76	60.31 (79)	50.06 (76)
34	69	57	60.00 (69)	48.81 (57)
35	83	83	58.15 (83)	48.34 (83)
36	13	13,25*	57.93(13)	45.72 (13,25)
37	7	21	57.12 (7)	45.28 (21)
38	57	36	54.78 (57)	44.71 (36)
39	45	45	54.60 (45)	44.25 (45)
40	21	64	52.27 (21)	40.96 (64)
41	14	65	52.14 (14)	39.64 (65)
42	65	37	50.00 (65)	37.02 (37)
43	8	7	48.00 (8)	36.92 (7)
44	64	8	47.25 (64)	36.53 (8)
45	78	14	46.06 (78)	35.24 (14)
46	17	17	45.40 (17)	34.87 (17)
47	11	63	44.47 (11)	34.58 (63)
48	16	30	44.33 (16)	33.87 (30)
49	37	16	42.86 (37)	32.80 (16)
50	39	39	42.00 (39)	32.61 (39)
51	63	11	41.14 (63)	31.59 (11)
52	80	23	39.53 (80)	30.80 (23)
53	23	78	36.24 (23)	29.33 (78)
54	20,30,82*	82	33.60 (20,30,82)	28.71 (82)
55	60	20	31.29 (60)	27.84 (20)

56	49	60	30.69 (49)	26.07 (60)
57	43	49	27.49 (43)	24.95 (49)
58	33	80	24.89 (33)	24.47 (80)
59	15	33	22.10 (15)	22.90 (33)
60	32	43	21.00 (32)	22.33 (43)
61	51	32	19.93 (51)	21.50 (32)
62	28	15	17.75 (28)	20.30 (15)
63	10	51	16.80 (10)	17.99 (51)
64	42	28	16.563(42)	17.61 (28)
65	34	10	15.75 (34)	16.93 (10)
66	66	42	14.76 (66)	16.15 (42)
67	31	34	13.39 (31)	15.50 (34)
68	9	66	10.65 (9)	14.60 (66)
69	5	31	8.055 (5)	13.47 (31)
70	68,77*	9	7.946 (68,77)	12.44 (9)
71	46	68,77*	6.632 (46)	10.10 (68,77)
72	74	5	5.676 (74)	10.01 (5)
73	27	46	4.421 (27)	7.461 (46)
74	35	35	3.600 (35)	7.440 (35)
75	29	74	3.316 (29)	7.338 (74)
76	40	27	2.182 (40)	5.380 (27)
77	4	29	1.105 (4)	4.503 (29)
78	38	40	1.077 (38)	2.730 (40)
79	-	4	-	2.149 (4)
80	-	38	-	1.314 (38)
81	-	-	-	-
82	-	-	-	-
83	-	-	-	-

*Species having the same average rank, constituting a weak order, therefore equal rank.

Note that the second and third columns of Table 1 are the same for the first eight ranks. They are, from the first to the eighth: *Bacillus licheniformis* ATCC 14580 (22), *Bacillus mucilaginosus* ACCC 10012 (24), *Pseudomonas* MGF-48 (50), *Bacillus subtilis* IAM 11062 (19), *Streptomyces* sp. (72), *Pseudomonas* sp. EPS-5028(48), *Actinomyces levoris* HUT 6156 (2) and *Arthrobacter nicotianae* IAM 12342 (6).

Because of the presence of some ties, i.e. same values in average ranks for some microorganisms, the last ranks in Table 1 are not available.

These results show that microorganism 22 (*Bacillus licheniformis* ATCC 14580) is the best U trapper. It belongs to the maximal objects (Fig. 6) and its order ideal $O(x)$ is pretty large (65 objects).

Bubley Dyer method is another helpful approach for ranking objects that generates a sample set of linear extensions from which average ranks can be calculated as in LPOM-methods.^[15] A detailed analysis of average ranks obtained by the application of this method shows that object 22 keeps at the top of the rank, which agrees with the average ranks calculated with LPOM-methods. Bubley Dyer calculations were run with the PyHasse software with a different number of Monte Carlo runs (ranging from one million to six millions) and samplings of linear extension (Data not shown).

If the maximal objects in the Hasse diagram are inspected, five out of eight are considered as well as good U trappers according to the top eight; these five microorganisms are 19, 22, 24, 50 and 72. This highlights the importance of average ranks for carrying out a decision-making process, in this case to know an ordering of objects in established positions, i.e. the first, the second, the third and so on.

3.3.2. FOU and ternary spaces of microorganisms

Table A3 (Supplementary material) shows posetic coordinates $|O(x)|$, $|I(x)|$ and $|F(x)|$ for each microorganism and the difference $|O(x)| - |F(x)|$.

The shapes of the set of points in Fig. 7a and 7b is strikingly similar. In general terms this follows from the fact that the FOU-space is a subset of the ternary space. In more details: In the FOU-space (Fig. 7a) the coordinates of the posetic cases of interest are: $A = (-82, 0)$; $B = (0, 82)$; $C = (82, 0)$; $D = (-41, 41)$; $E = (41, 41)$; $F = (0, 0)$ and $G = (0, 28)$.

Leftward-bottom region of Fig. 7a and 7b shows the objects having high $|F(x)|$, which are highly dominated species located in the neighbourhood of PCI A. Note that the line connecting PCI A with B in the FOU plot, location of minimal objects, split these species in one cluster with low I and another with high I. This shows that there are two sets of minimal microorganisms, with strong differences. They are, in fact, the minimal objects of the two components of the HD (Fig. 5). Maximal objects are also separated into two along the line connecting PCIs B with C. They also correspond to the maximal objects of the two components. Fig. 6 shows that there are several microorganisms that are better than others, close to be maximal; in contrast to the almost empty space around PCI D. Another empty region occurs for $F < O$ and low I. This shows the lack of strong

dominating species. The objects along the line connecting PCIs A and G correspond to species that are dominated by others but those that are close to G have better behaviour as U trappers. This trend is enhanced until meeting line BC. The spread of species near this line shows those microorganisms that behave better as U trappers but that are, in general, no better than most of the others, i.e. are not maximal. Note that there are more species near B than C, being C the best U trapper and B being the best and the worst at the same time because of its lack of comparabilities.

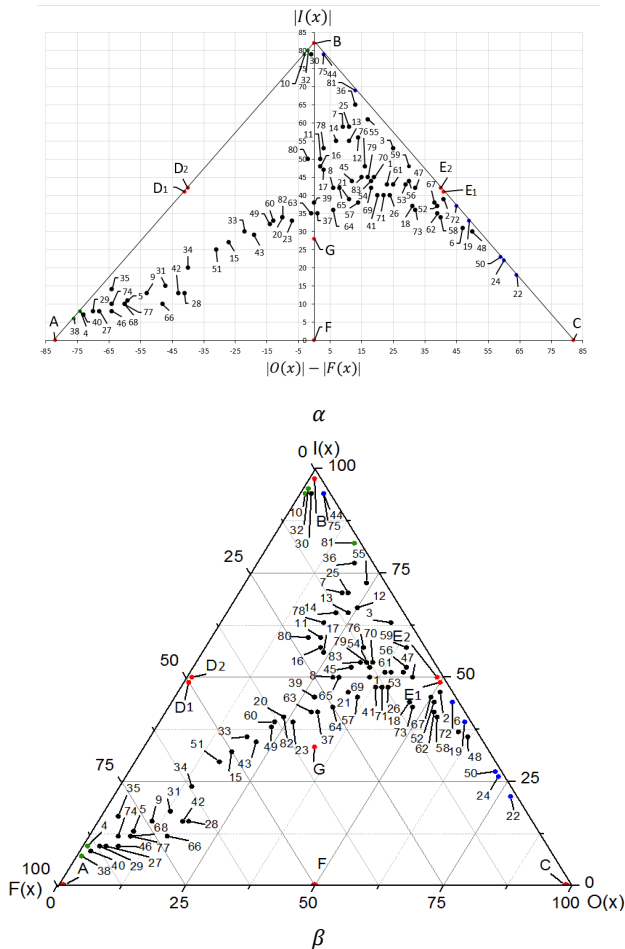


Figure 7. α) FOU and β) ternary plots of 83 microorganisms. Red points correspond to PCIs and green and blue ones to minimal and maximal objects, respectively.

3.3.3. Nearness of objects to posetic cases of interest

The assignment of object x to a PCI is given by the shortest distance of x to the PCIs. In case of ties x is considered as belonging to several PCIs. Results for the microorganism considered are summarised in Table 2.

Table 2. Posetic cases of interest (PCIs) and the microorganisms belonging to them.

PCI	PCI' name	Posetic coordinates	Label of microorganisms	Number of microorganisms
A	Maximally dominated	$ F(x) = 83$ $ O(x) = 1$ $ I(x) = 0$	4,5,27,29,35,38,40,46,68,74,77	11
B	Maximally incomparable	$ F(x) = 1$ $ O(x) = 1$ $ I(x) = 82$	7,10,12,14,25,30,32,36,44,55,75,81	12
C	Maximally dominating	$ F(x) = 1$ $ O(x) = 83$ $ I(x) = 0$	22	1
D1	Evenly dominated and incomparable	$ F(x) = 42$ $ O(x) = 1$ $ I(x) = 41$	9,15,28,31,34,42,51,66	8
D2		$ F(x) = 41$ $ O(x) = 1$ $ I(x) = 42$	-	0
E1*	Evenly dominating and incomparable	$ F(x) = 1$ $ O(x) = 42$ $ I(x) = 41$	2,6,19,24,48,50,52,58,62,67,72	11
E2		$ F(x) = 1$ $ O(x) = 41$ $ I(x) = 42$	1,3,18,26,41,47,53,54,56,59,61,69,70,71,73,76,79	17
F	Evenly dominated and dominating	$ F(x) = 42$ $ O(x) = 42$ $ I(x) = 0$	-	0
G	Evenly dominated, dominating and incomparable	$ F(x) = 28$ $ O(x) = 28$ $ I(x) = 28$	8,11,13,16,17,20,21,23,33,37,39,43,45,49,57,60,63,64,65,78,80,82,83	23

*In general, for maximal objects here located $|O(x)| > \{|F(x)|, |I(x)|\}$. Other objects have $|F(x)| < \{|O(x)|, |I(x)|\}$.

3.3.4. Comparison with HD, LPOM, FOU and ternary plots

From the HD (Fig. 6), maximal and minimal objects are visualised at the top or at the bottom. These positions highlight their dominating or dominated behaviour respectively. Likewise, Fig. 7 α and 7 β are depicting the position of maximal and minimal objects in specific PCIs; for example, C (22) and E (19,24,50,72) are gathering maximal objects with evenly dominating and incomparable behaviour.

In the case of object 22, its position is confirmed by their posetic characterisation (1,65,18), that leads to its location in PCI C. This means that microorganism 22 is the unique highly dominating object in this data matrix, explained by its highest $|O(x)|$ compared to the other objects in the poset.

According to their average ranks obtained from LPOM, other microorganisms occupying the next seven positions in the ordering are located in the nearness of PCI E, i.e., microorganisms 24, 50, 19, 72, 48, 2 and 6. PCI E represents evenly dominating and incomparable objects in such a way that they are characterised by high $|O(x)|$, ranging from 43 to 61, but having very low $|F(x)|$ i.e. ranging from 0 to 3, and high $|I(x)|$ (≤ 39) (see Table A3, Supplementary material).

As expected, this behaviour confirms their position at the top eight obtained by the application of LPOM (Table 2). Although in the nearness of PCI E, there are more microorganisms, not only those occupying the positions second to seventh at the top eight, the main differences are their very low number in $|F(x)|$ (3 to 11) and high $|I(x)|$ (36 to 53) accounting for their evenly dominating and incomparable behaviour (Table A3, Supplementary material).

Other maximal objects showed in Fig. 5 are located in the neighbourhood of PCI B pointing out their high value in $|I(x)|$ and their lack of complete dominance; these objects are 44 (1,4,79), 75 (1,4,79) and 81 (1,14,69). As expected, their behaviour would explain why they do not occupy the first positions in the ordering performed by LPOM (Table A3, Supplementary material).

In the case of minimal objects, it can be pointed out that according to their posetic characterisation, objects 10 (4,1,79) and 32 (3,1,80) have high degree of incomparabilities and are located in the PCI B. In contrast, objects 4 (75,1,8) and 38 (77,1,6), the other ones minimal objects, are located in the PCI A that gathers objects maximally dominated whose main posetic feature is that $|F(x)|$ is higher compared to $|F(x)|$ for other objects in the poset.

As seen, this posetic characterisation by using PCIs in FOU and ternary plots, confirms that in a HD, minimal objects are always either highly dominated or with high degree of incomparability.

4 Summary and discussion

We developed the idea of posetic coordinates and applied three mappings, focusing on the representation of FOU and ternary spaces. Findings can be summarised as in Fig. 8.

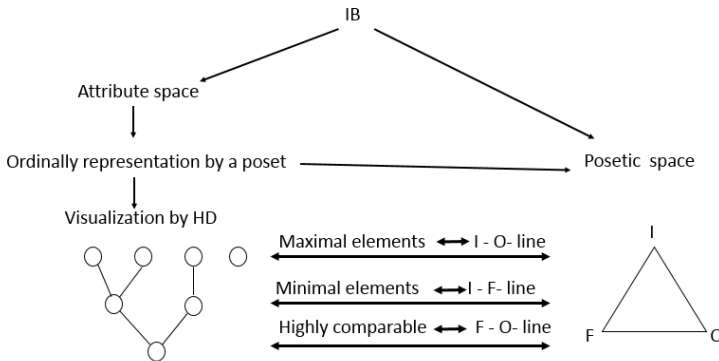


Figure 8. Relationships between attribute space and posetic space, where IB stands for information base, which gathers objects and attributes.

It can be hoped that by using different techniques of representation, maximal information can be extracted from the data set, keeping the very idea of the posetic nature of analysis. From the applicational point of view, it is found that out of 83 microorganisms, eight species are candidates for efficient uranium trapping. Results from LPOM show a top eight of microorganisms with high potential for removing U in aqueous systems, they are: *Bacillus licheniformis* ATCC 14580 (22), *Bacillus mucilaginosus* ACCC 10012 (24), *Pseudomonas* MGF-48 (50), *Bacillus subtilis* IAM 11062 (19), *Streptomyces* sp. (72), *Pseudomonas* sp. EPS-5028 (48), *Actinomyces levoris* HUT 6156 (2) and *Arthrobacter nicotianae* IAM 12342 (6).

Up to now we strictly separated the attribute space from the posetic space, nevertheless any mixture can be thought of, so for example supposed coordinates could be modified by metric information inherent in attributes. General mappings can have many other variants and this opens a field of further research.

Acknowledgements: N. Y. Quintero thanks Colciencias (Colombia) for the PhD. grant allowing her to carry out the current work (Convocatoria 617 de 2013. Doctorados nacionales). and Universidad de Pamplona and Universidad de Antioquia for the additional financial support. G. Restrepo thanks the Alexander von Humboldt Foundation/Stiftung and the Universidad de Pamplona for the support to conduct this research. The authors thank Professor P. Stadler at the Bioinformatics group at Leipzig University for allowing carrying out this study at his group and for facilitating all the needed conditions for its development.

Appendix

Proposition A1. For PCI D:

$$f(D) = \begin{cases} (X/2, 1, X/2), & \text{for even } |X| \text{ and} \\ \left(\left(\left\lfloor \frac{X}{2} \right\rfloor, 1, \left\lfloor \frac{X}{2} \right\rfloor \right) \text{ or} \right. & \\ \left. \left(\left\lfloor \frac{X}{2} \right\rfloor, 1, \left\lceil \frac{X}{2} \right\rceil \right) \right) & \text{for odd } |X|. \end{cases}$$

Proof: The condition $F = I$ of PCI D makes that O takes its minimum allowed value for x , i.e. $|O|=1$ (Proposition 2). From Theorem 1 it follows that

$$F + I = X \tag{A1}$$

As the condition requires $F = I$. This is realised for near values of F and I , then $F = I = X/2$.

For even X , F and $I \in \mathbb{N}$ (throughout the paper 0 is included as natural number), therefore $(F, O, I) = (X/2, 1, X/2)$.

For odd cases, given that F, O and $I \in \mathbb{N}$, to ensure that the resulting fraction also belong in \mathbb{N} , we consider different cases:

- i) $F = \lfloor X/2 \rfloor$, then by Equation A1 $I = X - \lfloor X/2 \rfloor = \lceil X/2 \rceil$,
- ii) $I = \lfloor X/2 \rfloor$, as in i it leads to $F = \lceil X/2 \rceil$.

Hence i leads to $(F, O, I) = (\lfloor X/2 \rfloor, 1, \lceil X/2 \rceil)$ and ii to $(\lceil X/2 \rceil, 1, \lfloor X/2 \rfloor)$ ■

Corollary A2: Either $(F, O, I) = (\lfloor X/2 \rfloor, 1, \lceil X/2 \rceil)$ or $(F, O, I) = (\lceil X/2 \rceil, 1, \lfloor X/2 \rfloor)$ are equivalent to (F, O, I) for $|X|$ even ■

Proof: As $\lfloor X/2 \rfloor + \lceil X/2 \rceil = X/2$ for even $|X|$, then

$$\begin{aligned} (\lfloor X/2 \rfloor, 1, \lceil X/2 \rceil) &= (\lceil X/2 \rceil, 1, \lfloor X/2 \rfloor) \\ &= (X/2, 1, X/2) \blacksquare \end{aligned}$$

Proposition A2: For PCI E:

$$f(E) = \begin{cases} (1, X/2, X/2), & \text{for even } |X| \text{ and} \\ \left(\left(1, \left\lfloor \frac{X}{2} \right\rfloor, \left\lfloor \frac{X}{2} \right\rfloor \right) \text{ or} \right. & \\ \left. \left(1, \left\lceil \frac{X}{2} \right\rceil, \left\lceil \frac{X}{2} \right\rceil \right) \right) & \text{for odd } |X|. \end{cases}$$

Proof: The condition $O = I$, following Proposition 2, leads to $O + I = X$, which makes that

$$(F, O, I) = \left(1, \frac{X}{2}, \frac{X}{2} \right), \text{ for } |X| \text{ even.}$$

When $|X|$ is odd, O and $I \notin \mathbb{N}$ and, as in Proposition 2, this leads to

i) $O = \lfloor X/2 \rfloor$, therefore $I = \lfloor X/2 \rfloor$,

ii) $I = \lceil X/2 \rceil$, therefore $O = \lceil X/2 \rceil$.

Which produces: $(F, O, I) = \left(1, \left\lfloor \frac{X}{2} \right\rfloor, \left\lfloor \frac{X}{2} \right\rfloor \right)$ or $(F, O, I) = \left(1, \left\lceil \frac{X}{2} \right\rceil, \left\lceil \frac{X}{2} \right\rceil \right)$ ■

Corollary A2: Either $(F, O, I) = \left(1, \left\lfloor \frac{X}{2} \right\rfloor, \left\lfloor \frac{X}{2} \right\rfloor \right)$ or $(F, O, I) = \left(1, \left\lceil \frac{X}{2} \right\rceil, \left\lceil \frac{X}{2} \right\rceil \right)$ are equivalent to (F, O, I) for $|X|$ even.

Proof: Likewise as in Corollary A1.

Proposition A3. For PCI F:

$$f(F) = \begin{cases} \left(\left(\left\lfloor \frac{X+1}{2} \right\rfloor, X - \left\lfloor \frac{X+1}{2} \right\rfloor + 1, 0 \right) \text{ or} \right. & \text{for even } |X| \text{ and} \\ \left. \left(X - \left\lfloor \frac{X+1}{2} \right\rfloor + 1, \left\lfloor \frac{X+1}{2} \right\rfloor, 0 \right) \right) & \\ \left(\frac{X+1}{2}, \frac{X+1}{2}, 0 \right), & \text{for odd } |X|. \end{cases}$$

Proof: PCI F brings the condition $F = O$, which makes that $|I| = 0$, therefore by Theorem 1:

$$F + O = X + 1 \tag{A2}$$

Near values of F and O make that

$$F = O = \frac{X+1}{2}$$

For $|X|$ odd, it can be expressed by $2n+1$, with $n \in \mathbb{N}$. Therefore $F = O = \frac{X+1}{2} = n + 1$,

which makes F and $O \in \mathbb{N}$.

Thus, for $|X|$ odd $(F, O, I) = \left(\frac{X+1}{2}, \frac{X+1}{2}, 0 \right)$.

For even $|X|$, it can be expressed by $2n$, with $n \in \mathbb{N}$. Hence, $F = O = \frac{X+1}{2} = \frac{2n+1}{2} \notin \mathbb{N}$.

To make F and O closer to each other as natural numbers, there are two possibilities:

i) $F = \left\lceil \frac{X+1}{2} \right\rceil$, then by Equation A2 $O = X - \left\lceil \frac{X+1}{2} \right\rceil + 1$.

ii) $O = \left\lceil \frac{X+1}{2} \right\rceil$, as in i, it leads to $F = X - \left\lceil \frac{X+1}{2} \right\rceil + 1$.

Thus, i leads to $(F, O, I) = \left(\left\lceil \frac{X+1}{2} \right\rceil, X - \left\lceil \frac{X+1}{2} \right\rceil + 1, 0 \right)$ and ii to

$$(F, O, I) = \left(X - \left\lceil \frac{X+1}{2} \right\rceil + 1, \left\lceil \frac{X+1}{2} \right\rceil, 0 \right) \blacksquare$$

Proposition A4. For PCI G:

$$f(G) = \left(\lfloor X/3 \rfloor, \lfloor X/3 \rfloor, X - 2 \left\lfloor \frac{X}{3} \right\rfloor + 1 \right).$$

Proof: PCI G requires $F = O = I$, which restricted initially to F and O makes that $F = O = X/3$. However, as $F, O \in \mathbb{N}$, then there are two options:

i) $F = O = \left\lfloor \frac{X}{3} \right\rfloor$

Which according to Theorem 1 leads to $I = X - 2 \left\lfloor \frac{X}{3} \right\rfloor + 1$.

ii) $F = O = \lfloor X/3 \rfloor$

That leads to $I = X - 2 \left\lfloor \frac{X}{3} \right\rfloor + 1$.

The full condition requires that, without loss of generality, either $I - F$ or $I - O$ attain minimum values.

For the case i, $I - F = X + 1 - \lfloor X/3 \rfloor$ and for ii $I - F = X + 1 - \lfloor X/3 \rfloor$. As $\lfloor X/3 \rfloor > \lfloor X/3 \rfloor$,

then $X + 1 - \left\lfloor \frac{X}{3} \right\rfloor < X + 1 - \lfloor X/3 \rfloor$, which makes case i be the minimum value.

Therefore

$$(F, O, I) = \left(\lfloor X/3 \rfloor, \lfloor X/3 \rfloor, X - 2 \left\lfloor \frac{X}{3} \right\rfloor + 1 \right) \blacksquare$$

Supplementary material

This information can be accessed in the following link:

<https://drive.google.com/open?id=1Hhze1oBkWLMLpc2BLupey95MdB2JEKJQ>

References

- [1] P. B. Sørensen, L. Carlsen, B. B. Mogesen, R. Bruggemann, B. Luther, S. Pudenz, U. Simon, E. Halfon, T. Bittner, K. Voigt, G. Welzl, F. Rediske, *Introduction to the General Principles of the Partial Order Ranking Theory, Order Theoretical Tools in Environmental Sciences*, Proceedings of the Second Workshop, Ministry of Environment and Energy National Environmental Research Institute, Roskilde, 2000, pp.1–172.
- [2] R. Bruggemann, L. Carlsen, *Partial Order in environmental Sciences and Chemistry*, Springer, Amsterdam, 2006, pp.1–399.
- [3] R. Bruggemann, G. Restrepo, Estimating octanol/water partition coefficients by order preserving mappings, *Croat. Chem. Acta.* **86** (2013) 509–517.
- [4] P. Bigus, S. Tsakovski, V. Simeonov, J. Namieśnik, M. Tobiszewski, Hasse diagram as a green analytical metrics tool: Ranking of methods for benzol[a]pyrene determination in sediments, *Anal. Bioanal. Chem.* **408** (2016) 3833–3841.
- [5] N. Y. Quintero, R. Bruggemann, G. Restrepo, Ranking of 38 prokaryotes according to their uranium uptake capacity in aqueous solutions: an approach from order theory through the Hasse diagram Technique, *Toxicol. Environ. Chem.* **99** (2017) 1242–1249.
- [6] W. T. Trotter, *Combinatorics and Partially Ordered Sets, Dimension Theory*, The Johns Hopkins Univ. Press, Baltimore, 1992.
- [7] W. L. Myers, G. P. Patil, Preliminary Prioritization based on partial order theory and R software for compositional complexes in landscape ecology, with applications to restoration, remediation, and enhancement, *Environ. Ecol. Stat.* **17** (2010) 411–436.
- [8] R. Bruggemann, L. Carlsen, K. Voigt, R. Wieland, PyHasse software for partial order analysis: scientific background and description of some modules, in: R. Bruggemann, L. Carlsen, J. Wittmann (Eds.), *Multi-Indicator Systems and Modelling in Partial Order*, Springer, New York, 2013, pp. 389–423.
- [9] G. Patil, W. L. Myers, R. Bruggemann, Multivariate datasets for inference of order: some considerations and explorations, in: R. Bruggemann, L. Carlsen, J. Wittmann (Eds.), *Multi-Indicator Systems and Modelling in Partial Order*, Springer, New York, 2014, pp.13–45.
- [10] G. A. Grätzer, *Lattice Theory: First Concepts and Distributive Lattices*, Dover, Mineola, 2009.
- [11] L. Carlsen, R. Bruggemann, An analysis of the ‘failed states index’ by partial order methodology, *J. Soc. Struct.* **14** (2013) 1–31.
- [12] D. West, *Ternary Equilibrium Diagrams*, Springer, New York, 2013.
- [13] J. D. MacCuish, N. E. MacCuish, *Clustering in Bioinformatics and Drug Discovery*, CRC Press, Boca Raton, 2011.
- [14] R. Bruggemann, L. Carlsen, An improved estimation of average ranks of partial orders, *MATCH Commun. Math. Comput. Chem.* **65** (2011) 383–414.
- [15] R. Bruggemann, P. Annoni, Average heights in partially ordered sets, *MATCH Commun. Math. Comput. Chem.* **71** (2014) 101–126.
- [16] R. Bubley, M. Dyer, Faster random generation of linear extensions, *Discr. Math.* **201** (1999) 81–88.
- [17] A. Nakajima, T. Tsuruta, Competitive biosorption of thorium and uranium by *micrococcus luteus*, *J. Radioanal. Nucl. Chem.* **260** (2004) 13–18.

- [18] A. Nakajima, T. Sakaguchi, Selective accumulation of heavy metals by microorganisms, *Appl. Microbiol. Biotechnol.* **24** (1986) 59–64.
- [19] T. Horikoshi, A. Nakajima, T. Sakaguchi, Studies on the accumulation of heavy metals elements in biological systems. XIX. Accumulation of uranium by microorganisms, *Eur. J. Appl. Microbiol. Biotechnol.* **12** (1981) 90–96.
- [20] C. Acharya, P. Chandwadkar, S. K. Apte, Interaction of uranium with a filamentous, heterocystous, nitrogen-fixing cyanobacterium, *Anabaena torulosa*, *Bioresour. Techn.* **116** (2012) 290–294.
- [21] T. Tsuruta, removal and recovery of uranium using microorganisms isolated from North American uranium deposits, *Am. J. Environ. Sci.* **3** (2007) 60–66.
- [22] S. Kulkarni, A. Ballal, S.K. Apte, Bioprecipitation of uranium from alkaline waste solutions using recombinant deinococcus radiodurans, *J. Hazard. Mat.* **262** (2013) 853–861.
- [23] Z. Yi, J. Yao, Kinetic and equilibrium study of uranium (VI) adsorption by *bacillus licheniformis*, *J. Radioanal. Nucl. Chem.* **293** (2012) 907–914.
- [24] Z. Yi, B. Lian, Adsorption of U (VI) by *bacillus mucilaginosus*, *J. Radioanal. Nucl. Chem.* **293** (2012) 321–329.
- [25] T. Tsuruta, Adsorption of uranium from acidic solution by microbes and effect of thorium on uranium adsorption by *streptomyces levoris*, *J. Biosci. Bioeng.* **97** (2004) 275–277.
- [26] D. Appukkuttan, C. Seetharam, N. Padma, A. S. Rao, S. K. Apte, PhoN-expressing, lyophilized, recombinant *deinococcus radiodurans* cells for uranium bioprecipitation, *J. Biotechnol.* **154** (2011) 285–290.
- [27] M. T. González-Muñoz, M. L. Merroun, N. Ben Omar, J. M. Arias, Biosorption of uranium by *myxococcus xanthus*, *Int. Biodeterior. Biodegrad.* **40** (1997) 107–114.
- [28] S. Choudary, P. Sar, Uranium Biomineralization by metal resistant *pseudomonas aeruginosa* strain isolated from contaminated mine waste, *J. Hazard. Mat.* **186** (2011) 336–343.
- [29] A. M. Marqués, X. Roca, M. D. Simon-Pujol, M. C. Fuste, F. Congregado, Uranium accumulation by *pseudomonas* sp. EPS-5028, *Appl. Microbiol. Biotechnol.* **35** (1991) 406–410.
- [30] F. Malekzadeh, A. Farazmand, H. Ghafourian, M. Shahamat, M. Levin, R. R. Colwell, Uranium accumulation by a bacterium isolated from electroplating effluent, *World J. Microbiol. Biotechn.* **18** (2002) 295–302.
- [31] A. Nakajima, T. Tsuruta, Competitive biosorption of thorium and uranium by action-mycetes, *J. Nucl. Sci. Techn.* **3** (2002) 528–531.
- [32] Z. Golab, B. Orlowska, R. W. Smith, Biosorption of lead and uranium by streptomyces sp., *Water Air Soil Pollut.* **60** (1991) 99–106.
- [33] C. Acharya, D. Joseph, S. K. Apte, Uranium sequestration by a marine cyanobacterium, *synechococcus elongatus* strain BDU/75042, *Bioresour. Technol.* **100** (2009) 2176–2181.
- [34] T. Reitz, A. Rossberg, A. Barkleit, S. Selenska-Pobell, M. L. Merroun, Decrease of U(VI) immobilization capability of the facultative anaerobic strain paenibacillus sp. JG-TB8 under anoxic conditions due to strongly reduced phosphatase activity, *PLoS One* **9** (2014) #e102447.
- [35] T. Reitz, M. Merroun, A. Rossberg, S. Selenska-Pobell, Interactions of *sulfolobus acidocaldarius* with uranium, *Radiochim. Acta.* **98** (2010) 249–257.